RESEARCH ARTICLE

Adaptive Finite-Time Attitude Control Based on Time-Varying Sliding Mode

Wei Pan[1], **Zitong Shen**[1], **Tianshuo Fang**[1], **Ruochen Tang**[1], **Rui Dai**[3], **Rui Xia**[4], **Yiyang Ni**[2] and **Quan Li**[2,*]

[1] Jiangsu Second Normal University, Nanjing 210013, China
[2] Institute of Artificial Intelligence Research, Jiangsu Second Normal University, Nanjing 210013, China
[3] College of Artificial Intelligence, Jiaxing University, Jiaxing 314001, China
[4] Independent Researcher, Guildford, United Kingdom

Abstract

This study investigates the finite-time attitude tracking problem of spacecraft. We employ finite-time control methods to develop a novel adaptive controller. The controller utilizes a time-varying non-singular adaptive fast terminal sliding mode. The time-varying sliding mode dynamically adjusts the sliding surface morphology. This adjustment enables precise control performance tuning. Additionally, adaptive methods estimate the upper bound of generalized disturbances. This estimation reduces the computational load of the controller. The proposed controller demonstrates high robustness against external disturbances and inertia uncertainties. Lyapunov methods prove the stability of the controller. Numerical simulations validate the effectiveness of the proposed control algorithm. The simulation results exhibit high precision and confirm the algorithm's performance.

Keywords: spacecraft attitude control, finite-time control, time-varying sliding mode, adaptive control.

1 Introduction

Space science and technology have developed rapidly in recent decades. Spacecraft including satellites and space stations serve critical functions in numerous on-orbit missions. These missions support both civilian and military applications. Various aerospace tasks, such as satellite reconnaissance, space-based measurements, pointing control, and scientific imaging, require precise spacecraft operations. Given these critical applications, spacecraft attitude control has emerged as a fundamental research topic [1].

Designing high-performance attitude controllers presents significant challenges. The controllers must achieve fast, reliable, and high-precision performance. This requirement has attracted considerable research attention in recent years [2].

Practical spacecraft attitude control faces multiple engineering constraints. External disturbances significantly impact control accuracy. These

Submitted: 08 December 2025
Accepted: 27 December 2025
Published: 25 January 2026

Vol. 1, **No.** 1, 2026.
10.62762/AEC.2025.182476

***Corresponding author:**
✉ Quan Li
quanli_1124@163.com

Citation
Pan, W., Shen, Z., Fang, T., Tang, R., Dai, R., Xia, R., Ni, Y., & Li, Q. (2026). Adaptive Finite-Time Attitude Control Based on Time-Varying Sliding Mode. *Aerospace Engineering Communications*, 1(1), 28–35.

disturbances include gravity gradients, solar radiation pressure, magnetic torque, and atmospheric drag. Additionally, system uncertainties complicate spacecraft dynamic behavior. These uncertainties arise from fuel consumption, payload deployment, and mass redistribution [4]. Inadequate compensation for these factors severely degrades system stability. Tracking performance also suffers significant deterioration. Therefore, ensuring high-precision and high-robustness attitude regulation remains challenging.

Researchers have proposed various solutions to address these challenges. Time-varying sliding mode techniques enable fault-tolerant attitude control. These methods achieve finite-time convergence. Smooth finite-time control methods suppress uncertainties, disturbances, and actuator faults. Several studies incorporate angular velocity constraints into attitude control design [6]. Terminal sliding-mode observers enhance fault-tolerant attitude tracking. Adaptive finite-time sliding-mode controllers reduce computational burden and improve robustness [7]. Several studies incorporate chattering reduction techniques to improve practical applicability of sliding mode control.

Finite-time control addresses increasingly stringent precision requirements. Response-time demands have also intensified [8–11]. Traditional terminal sliding-mode control suffers from singularity issues. Non-singular designs resolve these problems. The switching-function-based method in [12] exemplifies this approach. Researchers extended this method to decentralized and distributed spacecraft control problems [13, 14]. Neural-network-based adaptive control strategies effectively handle complex spacecraft dynamics [5]. Recent advances in adaptive learning control show significant promise. Self-learning control with tanh-type learning intensity demonstrates improved performance [15]. Online-learning control with weakened saturation response also enhances system capabilities [16, 17]. Compared with existing methods, the time-varying sliding mode offers distinct advantages by dynamically adjusting the convergence rate without requiring prior knowledge of disturbance bounds. Although this study focuses on spacecraft, the proposed method is applicable to general rigid-body systems.

This study proposes a novel adaptive spacecraft attitude control scheme. The scheme utilizes a time-varying sliding-mode structure. This structure effectively accommodates external disturbances and system uncertainties. We first construct a non-singular time-varying sliding surface. Subsequently, we develop a finite-time adaptive controller. Stability analysis demonstrates the theoretical foundation. Numerical simulations validate the proposed design effectiveness. The main contributions include:

(1) We propose a novel non-singular time-varying sliding surface. This surface enhances error-convergence characteristics. It avoids singularity issues in traditional terminal sliding-mode designs.
(2) We develop a finite-time adaptive control law. The adaptive sliding-mode structure provides enhanced design flexibility. Designers can tune transient performance and robustness without prior uncertainty bounds.
(3) We introduce a generalized-disturbance adaptive compensation mechanism. This mechanism estimates and counteracts lumped disturbances online. It reduces computational burden while maintaining high robustness against external perturbations and inertia uncertainties.

2 Spacecraft Model and Problem Description

This study employs specific mathematical notations. The symbols $\mathbb{R}^n$ and $\mathbb{R}^{n\times m}$ represent vectors and matrices in Euclidean space. Consider a vector $x \in \mathbb{R}^{3\times 1}$ defined as $x = [x_1, x_2, x_3]^T$. The power form is defined as $x^r \triangleq [x_1^r, x_2^r, x_3^r]^T$. The derivative of x^r follows:

$$(x^r)' \triangleq r \cdot \mathrm{diag}(x_1^{r-1}, x_2^{r-1}, x_3^{r-1})[\dot{x}_1, \dot{x}_2, \dot{x}_3]^T, \quad (1)$$

Additionally, the sign function is defined as:

$$\mathrm{sign}^2(x) \triangleq [\mathrm{sign}^2(x_1), \mathrm{sign}^2(x_2), \mathrm{sign}^2(x_3)]^T, \quad (2)$$

where $\mathrm{sign}^2(x_i) = |x_i|^2\mathrm{sign}(x_i)$.

We consider rigid spacecraft dynamics. The attitude kinematics and dynamics are described by:

$$J\dot{\omega} = -\omega^\times J\omega + u + d, \quad (3)$$

$$\begin{cases} \dot{q} = \frac{1}{2}(q_v^\times + q_0 I_3)\omega \\ \dot{q}_0 = -\frac{1}{2}q_v^T\omega \end{cases}. \quad (4)$$

The parameters in these equations have specific meanings. $J \in \mathbb{R}^{3\times 3}$ denotes the spacecraft inertia matrix. This matrix is positive definite. $\omega \in \mathbb{R}^3$

represents angular velocity. The velocity is expressed in the body-fixed coordinate system ($\mathcal{B}$). The inertial frame ($\mathcal{I}$) provides the reference frame. $u \in \mathbb{R}^3$ denotes the control input. $I_3 \in \mathbb{R}^{3\times3}$ represents the identity matrix. $d \in \mathbb{R}^3$ represents external disturbances.

The spacecraft attitude is described using unit quaternions. $(q_v \in \mathbb{R}^3, q_0 \in \mathbb{R})$ defines the attitude quaternion. Physically, q_v denotes the vector part aligned with the rotation axis, while q_0 represents the scalar part associated with the rotation angle. This quaternion represents the orientation of $\mathcal{B}$ relative to $\mathcal{I}$. Quaternion operations must satisfy the unit constraint:

$$q_v^T q_v + q_0^2 = 1. \tag{5}$$

For any vector $x \in \mathbb{R}^{3\times1}$, the skew-symmetric matrix is defined as:

$$x^\times = \begin{bmatrix} 0 & -x_3 & x_2 \\ x_3 & 0 & -x_1 \\ -x_2 & x_1 & 0 \end{bmatrix}. \tag{6}$$

The control target is specified by (q_v^d, q_0^d). Quaternion operations yield the error quaternion $(\tilde{q}, \tilde{q}_0)$. The error quaternion components are:

$$\tilde{q}_v = q_0^d q_v - (q_v^d)^\times q_v - q_0 q_v^d, \tag{7}$$

$$\tilde{q}_0 = (q_v^d)^T q_v + q_0^d q_0. \tag{8}$$

The error quaternion also satisfies the unit constraint $(\tilde{q}_i)^T \tilde{q}_i + (\tilde{q}_{0,i})^2 = 1$. The corresponding rotation matrix is:

$$R = (\tilde{q}_0^2 - \tilde{q}_v^T \tilde{q}_v) I + 2\tilde{q}_v \tilde{q}_v^T - 2\tilde{q}_0 \tilde{q}_v^\times. \tag{9}$$

The time-varying target signal is $\omega^d = \omega^d(t)$. This signal describes the coordinate system $\mathcal{D}$. The system $\mathcal{D}$ is defined relative to the inertial frame $\mathcal{I}$. The angular velocity error is therefore:

$$\tilde{\omega} = \omega - R\omega^d. \tag{10}$$

The error dynamics follow from the above equations:

$$J\dot{\tilde{\omega}} = -\omega^\times J\omega + J(\tilde{\omega}^\times R\omega^d - R\dot{\omega}^d) + u + d, \tag{11}$$

$$\begin{cases} \dot{\tilde{q}}_v = \frac{1}{2}(\tilde{q}_v^\times + \tilde{q}_0 I_3)\tilde{\omega} \\ \dot{\tilde{q}}_0 = -\frac{1}{2}\tilde{q}_v^T \tilde{\omega}_v \end{cases}. \tag{12}$$

The tracking problem is thus transformed into an error stabilization problem.

Assumption 2.1 External disturbances are bounded. ■

Assumption 2.2 $\left\|\omega^d\right\|_{\inf}$ and $\left\|\dot{\omega}^d\right\|_{\inf}$ are bounded. ■

Remark 1. External disturbances originate from multiple sources. Gravity, solar radiation, and magnetic forces are bounded. Air resistance is proportional to velocity squared. These disturbances satisfy the bound:

$$\|d\| \le c_1 + c_2 \|\omega\|^2, \tag{13}$$

where $c_1 \ge 0$ and $c_2 \ge 0$ are unknown constants. Spacecraft uncertainties also affect the control process. Fuel consumption causes parameter variations. Payload deployment and release induce additional uncertainties. These changes remain bounded. Reference [7] Section 3.2 provides detailed analysis. The generalized disturbances can be controlled by an upper bound. This bound relates to angular velocity and system constants.

3 Controller Design

3.1 Sliding Mode Design

We propose a novel sliding mode auxiliary variable:

$$s = \bar{J}[\tilde{\omega} + \alpha k^2(t)\tilde{q}_v + \beta k^2(t)\chi], \tag{14}$$

where $k(t)$ is the adaptive gain defined in Eq. (16). The function $\chi = \chi(\tilde{q}_v)$ is adapted from [12]. This piecewise formulation effectively circumvents the singularity problem inherent in conventional terminal sliding modes. This function exhibits the following structure:

$$\chi(\tilde{q}_v) = \begin{cases} \tilde{q}_v^r \\ \quad \text{if } \bar{s} = 0 \text{ or } \bar{s} \ne 0, \left|k^2(t)\tilde{q}_v\right| > \sigma \\ l_1\tilde{q}_v + l_2 \text{sign}^2(\tilde{q}_v) \\ \quad \text{if } \bar{s} \ne 0, \left|k^2(t)\tilde{q}_v\right| \le \sigma \end{cases}, \tag{15}$$

The design parameters have specific properties. α, β, and $r = r_1/r_2$ are positive constants. The integers r_1 and r_2 are positive and odd. They satisfy the constraint $0 < r < 1$. The parameter σ defines a small positive region. The adaptive gain $k(t)$ evolves according to:

$$\dot{k}(t) = \frac{-\gamma_0 k(t)}{1 + 4\gamma_0(1 - \tilde{q}_0)} \left\|\tilde{q}^T \tilde{\omega}\right\|. \tag{16}$$

The constant γ_0 is positive. Differentiating the sliding variable yields:

$$\begin{aligned} \dot{s} = \bar{J}[&\dot{\tilde{\omega}} + \alpha k^2(t)\dot{\tilde{q}} + \beta k^2(t)\dot{\chi}(\tilde{q}_v) \\ &+ 2\alpha k(t)\dot{k}(t)\tilde{q}_v + 2\beta k(t)\dot{k}(t)\chi(\tilde{q}_v)], \end{aligned} \tag{17}$$

The derivative of χ follows a piecewise structure:

$$\dot{\chi} = \dot{\chi}(\tilde{q}_v) = \begin{cases} r\,\mathrm{diag}\left(|q_1|^{r-1}, |q_2|^{r-1}, |q_3|^{r-1}\right)\dot{\tilde{q}}_v \\ \quad \text{if } \bar{s} = 0 \text{ or } \bar{s} \neq 0, \left|k^2(t)\tilde{q}_v\right| > \sigma \\ l_1\dot{\tilde{q}}_v + 2l_2\mathrm{diag}\left(|q_1|, |q_2|, |q_3|\right)\dot{\tilde{q}}_v \\ \quad \text{if } \bar{s} \neq 0, \left|k^2(t)\tilde{q}_v\right| \leq \sigma \end{cases}. \tag{18}$$

3.2 Adaptive Finite-Time Tracking Control

The control objective requires a robust adaptive law. We design the finite-time controller as:

$$u = -\tau_1 s - \tau_2 s^r - \tau_3 \mathrm{sign}(s) - \hat{\rho}\Phi \mathrm{sign}(s), \tag{19}$$

The control gains τ_1, τ_2, and τ_3 are positive constants. The function Φ is defined as:

$$\Phi \triangleq 1 + \|\omega\| + \|\omega\|^2, \tag{20}$$

This definition follows equations (25) and (26) in Section 3.2 of [7]. The adaptive parameter $\hat{\rho}$ evolves according to:

$$\dot{\hat{\rho}} = \xi\Phi\|s\|. \tag{21}$$

The adaptation gain ξ is positive.

3.3 Stability Analysis

Theorem 3.1 Under Assumptions 1 and 2, the spacecraft system achieves practical finite-time convergence to a small region around the target signal when controlled by the proposed adaptive law. ■

Proof: *We construct a composite Lyapunov function:*

$$V = \frac{1}{2}s^T s + 2k^2(t)(1-\tilde{q}_0) + \frac{k^2(t)}{2\gamma_0} + \frac{1}{2\xi}\tilde{v}^2. \tag{22}$$

Differentiating yields:

$$\begin{aligned}\dot{V} = s^T\bar{J}[&\dot{\tilde{\omega}} + \alpha k^2(t)\dot{\tilde{q}}_v + \beta k^2(t)\dot{\chi}(\tilde{q}_v) \\ &+ 2\alpha k(t)\dot{k}(t)\tilde{q}_v + 2\beta k(t)\dot{k}(t)\chi(\tilde{q}_v)] + \frac{1}{\xi}\tilde{v}\dot{\tilde{v}} \\ &+ 4k(t)\dot{k}(t)(1-\tilde{q}_0) + k^2(t)\tilde{q}_v^T\tilde{\omega} + \frac{k(t)\dot{k}(t)}{\gamma_0}\end{aligned}. \tag{23}$$

This expression can be reformulated as:

$$\begin{aligned}\dot{V} = s^T[v_e + v_k + u + d] + \frac{1}{\xi}\tilde{v}\dot{\tilde{v}} + k^2(t)\tilde{q}_v^T\tilde{\omega} \\ + \frac{k(t)\dot{k}(t)}{\gamma_0}[1 + 4\gamma_0(1-\tilde{q}_0)]\end{aligned}, \tag{24}$$

where the auxiliary terms are:

$$v_e = -\omega^\times J\omega + J(\tilde{\omega}^\times R\omega^d - R\dot{\omega}^d), \tag{25}$$

$$\begin{aligned}v_k =&\alpha k^2(t)J\dot{\tilde{q}} + \beta k^2(t)J\dot{\chi}(\tilde{q}_v) + 2\alpha k(t)\dot{k}(t)J\tilde{q} \\ &+ 2\beta k(t)\dot{k}(t)J\chi(\tilde{q})\end{aligned}. \tag{26}$$

Substituting the control law and applying the disturbance bound yields:

$$\begin{aligned}\dot{V} \leq&(\rho - \hat{\rho})\Phi\|s\| - \tau_1 s^T s - \tau_2 s^T s^r \\ &- \tau_3 s^T sign(s) + \tilde{\rho}\Phi\|s\| \\ \leq&0\end{aligned}. \tag{27}$$

The condition $\tau_3 \geq \tilde{\rho}$ ensures $\dot{V} \leq 0$, establishing asymptotic stability.

To prove finite-time convergence to the sliding surface, consider the Lyapunov function:

$$V = \frac{1}{2}s^T s. \tag{28}$$

Its derivative satisfies:

$$\begin{aligned}\dot{V}(s) \leq&(\tilde{\rho} - \tau_3)\|s\| - \tau_1\|s\|^2 - \tau_2 s^T s^r \\ \leq& -\delta_1 V(s) - \delta_2 V^{\frac{1+r}{2}}(s)\end{aligned}, \tag{29}$$

where $\delta_1, \delta_2 > 0$ are constants. By Lemma 2.2 in [13], the system reaches the sliding surface in finite time.

We analyze two convergence scenarios:

Case 1: *When $\bar{s}_i \neq 0$ and $\left|k^2(t)\tilde{q}_i\right| \leq \sigma$, the system has converged to a small region. The error bound becomes:*

$$\begin{aligned}|\tilde{\omega}_i| \leq&k^2(t)[\alpha|\tilde{q}_i| + \beta(l_1|\tilde{q}_i| + l_2|sign^2(\tilde{q}_i)|)] \\ \leq&k^2(t)(\alpha\sigma + \beta\sigma^r)\end{aligned}. \tag{30}$$

Thus $\tilde{\omega}_i$ and $k^2(t)\tilde{q}_i$ converge to a small region in finite time.

Case 2: *When $\bar{s}_i = 0$, the sliding condition yields:*

$$\tilde{\omega}_i + \alpha k^2(t)\tilde{q}_i + \beta k^2(t)\tilde{q}_i^r = 0. \tag{31}$$

This directly implies finite-time convergence of $\tilde{\omega}_i$ and $k^2(t)\tilde{q}_i$.

The adaptive parameter behavior follows the analysis in Theorem 1.1 of [13]. Consequently, the estimation errors imply that the system achieves practical finite-time convergence to a small residual set.

■

3.4 Modified Adaptive Finite-Time Tracking Control

Since the controller design in Section 3.2 introduces the sign function, which causes chattering, to reduce the chattering phenomenon, continuous functions are often used to replace the sign function, commonly including boundary layer methods, hyperbolic tangent functions, etc [3]. In this section, we use the hyperbolic tangent function method to reduce chattering. Therefore, the controller can be written as

$$u = -\tau_1 s - \tau_2 s^r - \tau_3 \tanh(\frac{s}{\lambda}) - \hat{\rho}\Phi \tanh(\frac{s}{\lambda}), \quad (32)$$

where λ is a positive constant.

4 Numerical Simulation

This section presents comprehensive simulation results to validate the proposed control algorithm. We first specify spacecraft and controller parameters, then analyze the closed-loop performance. The actuator input is limited to 2 Nm, reflecting practical spacecraft constraints.

4.1 Parameter Configuration

The spacecraft inertia matrix is selected as:

$$\bar{J} = \begin{bmatrix} 20 & 2 & 0.9 \\ 2 & 17 & 0.5 \\ 0.9 & 0.5 & 15 \end{bmatrix}. \quad (33)$$

To simulate realistic operating conditions, we introduce time-varying inertia fluctuations following [7]:

$$\begin{aligned} \Delta J =& \text{diag}(8,7,6)e^{-0.1t} - \text{diag}(1,1,1)h(4) \\ &+ \text{diag}(\sin(0.5t), \cos(0.5t), \sin(0.5t)) \end{aligned}, \quad (34)$$

where $h(\cdot)$ represents a step function modeling sudden parameter changes at $t = 4$ seconds.

The external disturbance is modeled as:

$$d(t) = [0.01\sin(0.4t), 0.05\cos(0.5t), 0.08\cos(0.7t)]^T. \quad (35)$$

Initial conditions are specified as:

$$q^d(0) = [1,0,0,0]^T, \quad (36)$$

$$\tilde{q}(0) = [0.8762, 0.3, -0.2, 0.2]^T, \quad (37)$$

$$\omega^d(t) = 0.05[\cos(t/10), -\sin(t/10), -\cos(t/10)]^T. \quad (38)$$

Controller parameters are carefully tuned: $k(0) = 1, \alpha = 1.2, \beta = 0.1, r = 3/5, \sigma = 0.05, \gamma_0 = 0.5, \tau_1 = 1, \tau_2 = 0.1, \tau_3 = 0.1, \rho = 0.1, \xi = 0.0005, \lambda = 0.01$.

4.2 Performance Analysis

Figures 1, 2, 3, 4, 5, and 6 demonstrate the closed-loop performance under coupled inertia uncertainties and external disturbances. The sliding variables in Fig. 1 exhibit rapid convergence to a small neighborhood of zero, confirming effective error damping and fast attraction to the sliding manifold. This favorable behavior extends to state responses: both attitude-error quaternion (Fig. 2) and angular-velocity error (Fig. 3) show smooth, monotonic convergence. The control torques (Fig. 4) remain continuous without high-frequency oscillations, validating the chattering suppression capability of the continuous switching design. The adaptive parameters $k(t)$ (Fig. 5) and $\hat{\rho}(t)$ (Fig. 6) converge to steady values, demonstrating coordinated controller adaptation throughout the maneuver. The smooth control torque profiles confirm that the proposed method effectively mitigates chattering while maintaining precise tracking.

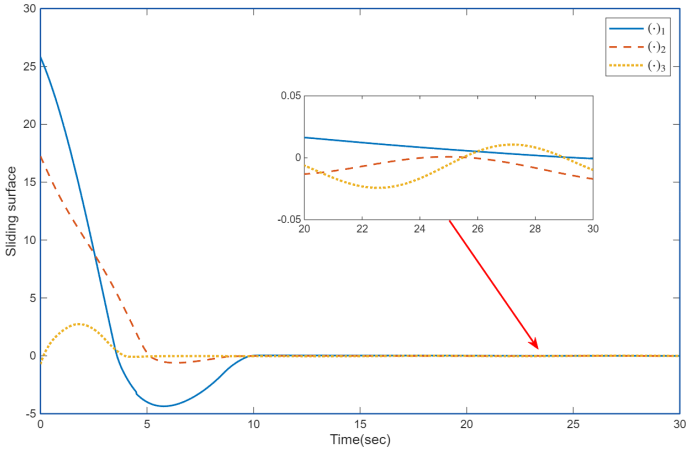

Figure 1. Time response of the sliding surface vector $(s = [s_1, s_2, s_3]^T)$.

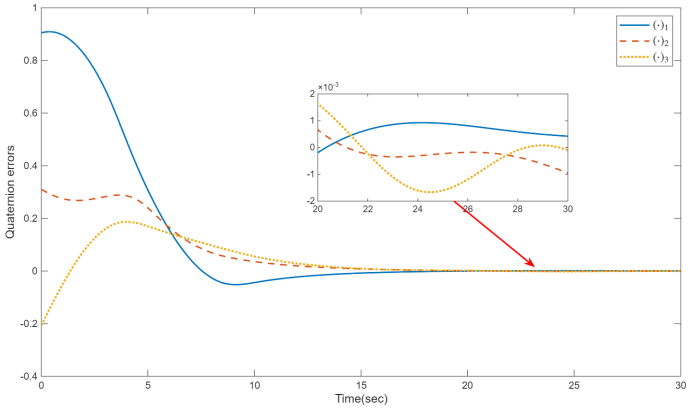

Figure 2. Evolution of the attitude error vector $(\tilde{q}_v = [\tilde{q}_{v1}, \tilde{q}_{v2}, \tilde{q}_{v3}]^T)$.

The behaviors observed across these figures highlight the underlying mechanisms and advantages of the proposed design. The rapid reduction of

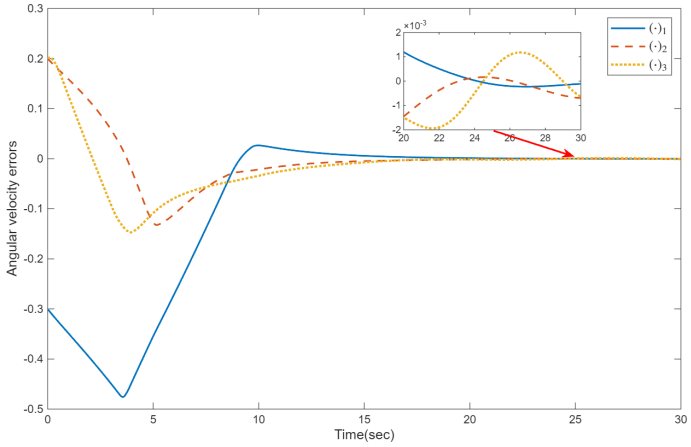

Figure 3. Angular velocity tracking error ($\tilde{\omega} = [\tilde{\omega}_1, \tilde{\omega}_2, \tilde{\omega}_3]^T$).

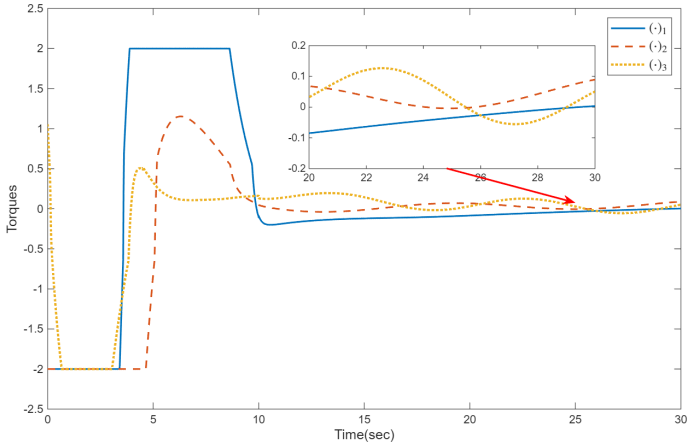

Figure 4. Control torque output ($\mu = [\mu_1, \mu_2, \mu_3]^T$).

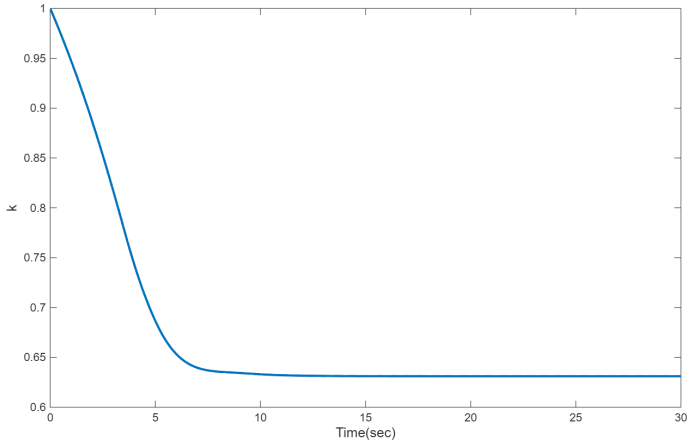

Figure 5. Time evolution of the adaptive gain ($k(t)$).

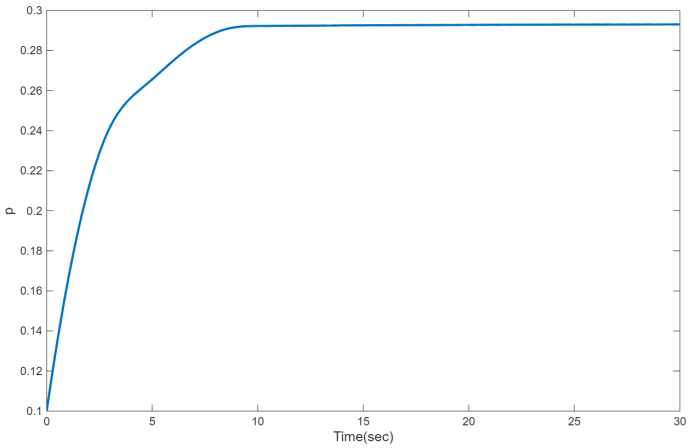

Figure 6. Estimation of the generalized disturbance upper bound ($\hat{\rho}(t)$).

sliding variables confirms that the redesigned sliding surface enforces strong finite-time error attenuation. The smooth convergence of both quaternion and angular-velocity errors demonstrates the effectiveness of the continuous switching structure, which eliminates the discontinuities inherent in traditional sliding-mode approaches. The bounded and chattering-free control input further shows that this modification directly improves actuator-level implementability. Moreover, the complementary evolution of $k(t)$ and $\hat{\rho}(t)$ with the gain decreasing as tracking improves while the disturbance estimate increases to compensate external perturbations reveals the controller's key innovation: disturbance rejection and gain adaptation operate in a coordinated manner without requiring prior knowledge of uncertainty bounds. This interaction between the adaptive laws and sliding-mode dynamics explains the controller's ability to maintain smooth transients, avoid excessive control effort, and achieve robust performance under coupled uncertainties.

5 Conclusion

This study presents a novel adaptive finite-time attitude control scheme for spacecraft operating under coupled inertia uncertainties and external disturbances. The proposed method integrates a time-varying non-singular sliding surface with adaptive compensation mechanisms to achieve robust performance. Rigorous theoretical analysis demonstrates finite-time convergence stability, while comprehensive simulations validate the practical effectiveness.

The key innovations and achievements include: (1) A non-singular time-varying sliding surface that

enhances convergence characteristics while avoiding traditional singularity problems; (2) An adaptive control law providing flexible tuning of transient performance without requiring prior uncertainty bounds; (3) A generalized-disturbance compensation mechanism that reduces computational burden while maintaining robustness.

Simulation results confirm that the controller achieves high-precision attitude tracking, strong disturbance rejection, and finite-time convergence under realistic operating conditions. The control torques remain continuous and chattering-free, demonstrating practical implementability. The adaptive parameters exhibit coordinated evolution, effectively balancing performance requirements with robustness needs.

The proposed approach offers significant theoretical contributions to spacecraft control literature and demonstrates substantial practical applicability for complex space missions. Future work could explore extension to formation flying control and integration with fault-tolerant mechanisms.

Data Availability Statement

Data will be made available on request.

Funding

This work was supported by the National Natural Science Foundation of China under Grant 62471204, and Jiangsu Provincial Key Research and Development Program under Grant BE2023022-2.

Conflicts of Interest

The authors declare no conflicts of interest.

AI Use Statement

The authors declare that no generative AI was used in the preparation of this manuscript.

Ethical Approval and Consent to Participate

Not applicable.

References

[1] Yin, S., Xiao, B., Ding, S. X., & Zhou, D. (2016). A review on recent development of spacecraft attitude fault tolerant control system. *IEEE Transactions on Industrial Electronics, 63*(5), 3311-3320. [CrossRef]

[2] Hu, Q., Chen, W., Guo, L., & Biggs, J. D. (2021). Adaptive fixed-time attitude tracking control of spacecraft with uncertainty-rejection capability. *IEEE Transactions on Systems, Man, and Cybernetics: Systems, 52*(7), 4634-4647. [CrossRef]

[3] Suleiman, H. U., Mu'azu, M. B., Zarma, T. A., Salawudeen, A. T., Thomas, S., & Galadima, A. A. (2018, August). Methods of chattering reduction in sliding mode control: a case study of ball and plate system. In *2018 IEEE 7th international conference on adaptive science & technology (ICAST)* (pp. 1-8). IEEE. [CrossRef]

[4] Thakur, D., Srikant, S., & Akella, M. R. (2015). Adaptive attitude-tracking control of spacecraft with uncertain time-varying inertia parameters. *Journal of guidance, control, and dynamics, 38*(1), 41-52. [CrossRef]

[5] Levant, A., & Fridman, L. (2004). Robustness issues of 2-sliding mode control. *Variable structure systems: from principles to implementation, 66*, 131.

[6] Zhu, Y., Ning, X., Wang, S., & Wang, Z. (2024). Fixed-time fuzzy disturbance observer–based adaptive integral sliding-mode spacecraft attitude control under time-varying output constraints. *Proceedings of the Institution of Mechanical Engineers, Part I: Journal of Systems and Control Engineering, 238*(5), 779-790. [CrossRef]

[7] Guo, Z., Wang, Z., & Li, S. (2022). Global finite-time set stabilization of spacecraft attitude with disturbances using second-order sliding mode control. *Nonlinear Dynamics, 108*(2), 1305-1318. [CrossRef]

[8] Xiao, B., Hu, Q., & Zhang, Y. (2014). Finite-time attitude tracking of spacecraft with fault-tolerant capability. *IEEE Transactions on Control Systems Technology, 23*(4), 1338-1350. [CrossRef]

[9] Zhao, L., & Jia, Y. (2015). Finite-time attitude tracking control for a rigid spacecraft using time-varying terminal sliding mode techniques. *International Journal of Control, 88*(6), 1150-1162. [CrossRef]

[10] Sun, S., Zhao, L., & Jia, Y. (2016). Finite-time output feedback attitude stabilisation for rigid spacecraft with input constraints. *IET Control Theory & Applications, 10*(14), 1740-1750. [CrossRef]

[11] Shao, X., & Hu, Q. (2016, July). Adaptive finite-time attitude tracking control for rigid spacecraft with actuator saturation constraints. In *2016 35th Chinese Control Conference (CCC)* (pp. 3321-3326). IEEE. [CrossRef]

[12] Hu, Q., & Shao, X. (2016). Smooth finite-time fault-tolerant attitude tracking control for rigid spacecraft. *Aerospace Science and Technology, 55*, 144-157. [CrossRef]

[13] Zhou, N., Xia, Y., Wang, M., & Fu, M. (2015). Finite-time attitude control of multiple rigid spacecraft using terminal sliding mode. *International Journal of Robust and Nonlinear Control, 25*(12), 1862-1876. [CrossRef]

[14] Zhou, N., Xia, Y., Lu, K., & Li, Y. (2015). Decentralised finite-time attitude synchronisation and tracking control for rigid spacecraft. *International Journal of Systems Science, 46*(14), 2493-2509. [CrossRef]

[15] Zhang, C., Lu, W., Zhao, S., Wu, J., Zhu, X., Liu, Z., & He, W. (2024). Enhancing attitude tracking with self-learning control using tanh-type learning intensity. *IEEE Transactions on Automation Science and Engineering, 22*, 16976–16986. [CrossRef]

[16] Zhang, C., Ahn, C. K., Wu, J., & He, W. (2024). Online-learning control with weakened saturation response to attitude tracking: A variable learning intensity approach. *Aerospace Science and Technology, 117*, 106981. [CrossRef]

[17] Lewis, F. L., & Vrabie, D. (2009). Reinforcement learning and adaptive dynamic programming for feedback control. *IEEE circuits and systems magazine, 9*(3), 32-50. [CrossRef]

Quan Li received the Ph.D. degree in Control Science and Engineering from Jiangnan University, Wuxi 21400, Jiangsu, China, in 2025. (Email: quanli_1124@163.com)